Atomistic Simulations of Phosphatidylcholines and Cholesteryl Esters in High-Density Lipoprotein-Sized Lipid Droplet and Trilayer: Clues to Cholesteryl Ester Transport and Storage

Artturi Koivuniemi,[†‡] Mikko Heikelä,[§] Petri T. Kovanen,[‡] Ilpo Vattulainen,[†§¶] and Marja T. Hyvönen[‡§‖*]

[†]Department of Physics, Tampere University of Technology, Tampere, Finland; [‡]Wihuri Research Institute, Helsinki, Finland; [§]Department of Applied Physics, Helsinki University of Technology, Helsinki, Finland; [¶]MEMPHYS Center for Biomembrane Physics, University of Southern Denmark, Odense, Denmark; and [‖]Department of Physical Sciences, University of Oulu, Oulu, Finland

ABSTRACT Cholesteryl esters (CEs) are the water-insoluble transport and storage form of cholesterol. For both transport and storage, phospholipids and proteins embrace the CEs to form an amphipathic monolayer that surrounds the CEs. CEs are transported extracellularly in lipoproteins and are stored intracellularly as cytoplasmic lipid droplets. To clarify the molecular phenomena related to the above structures, we conducted atomistic molecular-dynamics simulations for a spherical, approximately high density lipoprotein sized lipid droplet comprised of palmitoyl-oleoyl-phosphatidylcholine (POPC) and cholesteryl oleate (CO) molecules. An additional simulation was conducted for a lamellar lipid trilayer consisting of the same lipid constituents. The density profiles showed that COs were located in the core of the spherical droplet. In trilayer simulations, CO molecules were also in the core and formed two denser strata. This is remarkable because the intra- and intermolecular behaviors of the COs were similar to previous findings from bulk COs in the fluid phase. In accordance with previous experimental studies, the solubility of COs in the POPC monolayers was found to be low. The orientation distribution of the sterol moiety with respect to the normal of the system was found to be broad, with mainly isotropic or slightly parallel orientations observed deep in the core of the lipid droplet or the trilayer, respectively. In both systems, the orientation of the sterol moiety changed to perpendicular with respect to the normal close to the phopsholipid monolayers. Of interest, within the POPC monolayers, the intramolecular conformation of the COs varied from the previously proposed horseshoe-like conformation to a more extended one. From a metabolic point of view, the observed solubilization of CEs into the phospholipid monolayers, and the conformation of CEs in the phospholipid monolayers are likely to be important regulatory factors of CE transport and hydrolysis.

INTRODUCTION

Cholesteryl ester (CE) molecules are the transport and storage form of cholesterol molecules both extra- and intracellularly (1). Extracellularly, CE molecules are mainly transported inside lipoprotein particles and are thus strongly related to the development of atherosclerosis, the main cause of cardiovascular disease. The initial sign of cholesterol accumulation in atherosclerosis is the appearance of lipid droplets and vesicles within the extracellular matrix of the arterial intima. The features and composition of these structures suggest their origin from low-density lipoprotein (LDL) particles (2). The next sign of cholesterol accumulation in atherosclerosis is the appearance of cytoplasmic lipid droplets in macrophages present in the atherosclerosis-prone areas of the arterial wall. These droplets are composed mainly of cholesteryl oleate (CO), a cholesterol component derived from modified (e.g., oxidized) LDL particles that have been taken up by the macrophages (3). Such lipid-filled macrophages are called foam cells, and they are the hallmark of atherogenesis. The cytoplasmic CE droplets are metabolically active in that the esters they contain are continuously hydrolyzed to yield unesterified cholesterol and unesterified fatty acids, after which the liberated cytoplasmic cholesterol is reesterified and incorporated into the droplets (1,4). Conversion of the foam cells back to macrophages is possible if efflux of the unesterified cholesterol molecules is induced by adding cholesterol acceptors (notably the various components of the high-density lipoprotein (HDL) fraction) to the culture medium in which the foam cells are grown, or if such acceptors are injected into the circulation of atherosclerotic animals (5,6). However, although the proteomics of lipid droplets has gained considerable attention lately (7), the characteristics of the lipid compartment have remained largely elusive.

In both transport and storage, the CE molecules are encapsulated by amphiphilic phospholipid molecules that ensure the water solubility of the systems by forming colloidal particles (2,8). The chemical and physical properties of CEs differ from those of unesterified cholesterol. The solubility of CEs into a phospholipid monolayer has been shown to be much less than the solubility of cholesterol molecules, as the CE molecules form separate oil or liquid crystalline phases in the presence of phospholipids (9,10). However, it has been shown that small amounts of CEs are solubilized into phospholipid bilayers, and that the amount depends on the composition of the phospholipids (9,11). This is an important aspect from a metabolic point of view because the availability of CEs, along with the conformation of CEs at the phospholipid-water interfaces, may be crucial for the

Submitted October 23, 2008, and accepted for publication January 14, 2009.

*Correspondence: marja.hyvonen@oulu.fi

Editor: Gregory A. Voth.

0006-3495/09/05/4099/10 $2.00

doi: 10.1016/j.bpj.2009.01.058

exchange and hydrolysis of CEs, which are catalyzed by proteins. Thus, the phospholipid monolayer surrounding lipoproteins can also be seen as a regulator of CE transportation and hydrolysis. In addition, the physical state of the CE phases has been shown to affect their availability to be cleared from the cytoplasm of cells (12) and from atherosclerotic plaques (13). In light of the above-mentioned aspects, and the fact that both extra- and intracellular lipid droplets play a major role in the initiation of cardiovascular diseases, it is of central interest to probe the molecular- and atomic-level characteristics of related molecular systems.

Atomic-resolution information regarding lipoproteins, especially the large ones, is limited. This is mainly due to the complexity of supramolecular lipoprotein assemblies of proteins and lipids, which is evident in many ways. First, the length scales of lipoproteins are of the order of 10 nm, which renders experimental determination of lipoprotein structures very difficult. Second, since the structures of lipoproteins and lipid droplets are dynamic due to thermal fluctuations, experiments can at best only provide snapshots of transient structures. Third, the above points highlight the fact that studies of the dynamics of these complex systems take place over timescales as short as nanoseconds, which also presents a challenge for experiments. Therefore, the complexity of lipoproteins and lipid droplets makes it highly challenging to apply experimental structural biology methodologies.

An alternate approach is to complement experiments with the use of atomistic simulations, which enable investigators to study relatively large molecular systems in atomic detail, including their dynamics. Further, the development of coarse-grained models is allowing them to cover considerably larger scales in time and space, and in some recent studies coarse-grained models were successfully applied to lipoprotein models (14–17). However, due to the lack of atomic-scale information regarding lipoproteins and related lipid droplet particles, in this study we chose to employ the ''bottom-up strategy'' whereby we first apply atomic-resolution models to gain insight into the lipoprotein properties, and use that information to construct coarse-grained descriptions of these complex systems (to be presented elsewhere).

We chose to use CO and 1-palmitoyl-2-oleoyl-*sn*-glycero-3-phosphatidylcholine (POPC) as the most suitable components of our model to address questions regarding lipid droplets and lipoproteins. This choice is supported by the fact that CO is the most prevalent CE in intracellular storage (18) and also abundant in the transport process inside the lipoproteins (2). POPC, in turn, is one of the most common physiological PCs, and has also been found to be prevalent in the surface layer of lipid droplets (8). Furthermore, POPC is one of the most investigated PCs, both experimentally and in computational simulation studies of model lipid systems.

We simulated a molecular system of 180 POPC and 35 CO molecules forming a spherical, HDL-sized lipid droplet in aqueous solvent. To characterize effects due to size and different curvatures, we also constructed a planar lipid trilayer system containing 128 POPC and 199 CO molecules in excess water. These two-component systems provide what we believe are new insights into the molecular organization and dynamics of lipid droplets and lipoproteins. Our study was facilitated by recent work on isotropic bulk systems of CO molecules and models of POPC bilayers (19,20). The analysis of the simulation data focused on the solubility of CO molecules into the POPC monolayer, as well as on the distribution and conformation of COs in the systems. The intra- and intermolecular properties of CO molecules were compared with results from previous simulations of bulk CO molecules. In addition, the POPC molecules were analyzed and the results were compared with those from previous simulations of POPC bilayers.

MATERIALS AND METHODS

Initial structures and simulations

To construct a spherical-like core of the droplet, we extracted 35 COs from the end of the preequilibrated simulation of the isotropic CO system (20). A monolayer of 180 POPCs was wrapped around the CO core. The ratio of phospholipids and core lipids in our lipid droplet is somewhat larger than that in actual lipoproteins because in this work we had no apoA-Is shielding some of the phospholipids at the surface (21). We added excess water to the system of cubic shape with dimensions of $12 \times 12 \times 12$ nm^3. Water molecules overlapping lipids were removed, after which there were 171 water molecules per POPC molecule in the system. This was followed by energy minimization using the steepest-descent algorithm.

For the trilayer system, periodic copies of our bulk CO system were utilized to obtain 199 preequilibrated CO molecules in a box with dimensions of ~$8 \times 8 \times 6$ nm^3. The initial trilayer was constructed by combining the CO system with a preequilibrated POPC bilayer (22) (available at http://moose.bio.ucalgary.ca). The box of COs was placed between two POPC monolayers. After the system was hydrated, water molecules that overlapped the lipids were removed (yielding 44 waters per POPC), resulting in system dimensions of ~$8 \times 8 \times 13$ nm^3. Finally, the energy of the trilayer system was minimized by the steepest-descent algorithm.

The molecular-dynamics simulations were performed with the use of GROMACS 4.0 Beta (23). The force-field and simulation parameters used in this study are given in the Supporting Material. For both the droplet and trilayer systems, we first carried out short (500 ps) simulations with lipid molecules frozen in all x, y, and z dimensions to relax the water molecules around the lipids. These structures were then used as initial structures in the simulations. The lipid droplet system was simulated for 90 ns and the trilayer simulation was 160 ns. The molecular structures of POPC and CO are sketched in Fig. 1 and the initial simulation structures for the droplet and trilayer systems are shown in Fig. 2.

Additionally, for comparison purposes a preequilibrated POPC bilayer of 128 lipids (22) (available at http://moose.bio.ucalgary.ca) was used to perform a 20 ns simulation with the same force field and other simulation details.

Data analysis

To generate two-dimensional (2D) number-density maps (also called an axial-radial number-density map) for the droplet system, we first chose a 2 nm slice (in the z direction) centered on the center of mass (COM) of the droplet. We then calculated the radial densities of the atoms and POPC molecules in the slice by using 0.02 nm bins around the COM of the droplet. The averaging direction was the z axis.

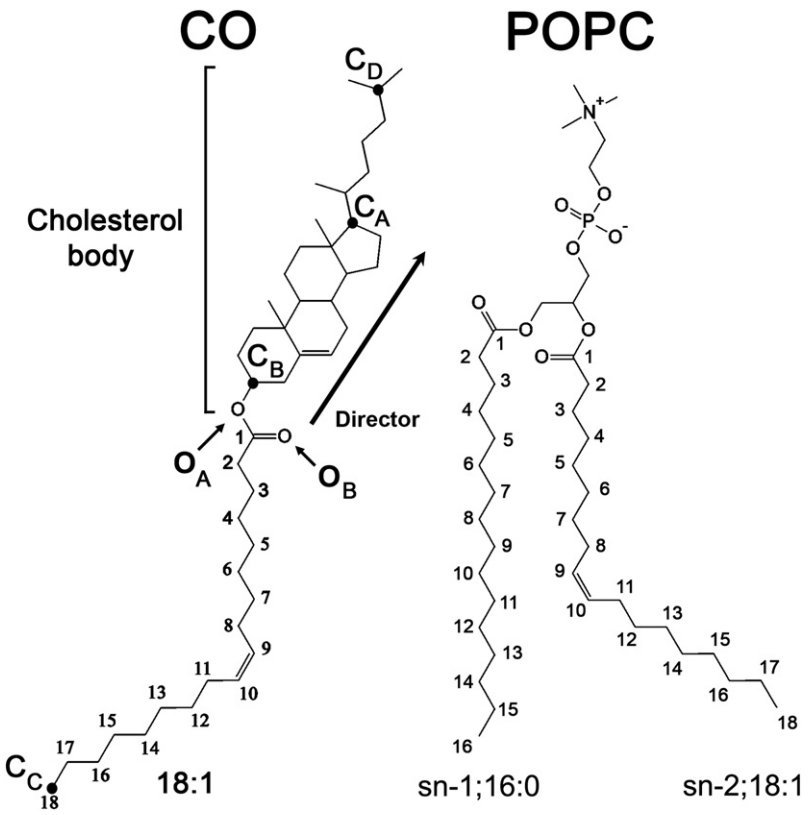

FIGURE 1 Molecular structures and atom labeling for CO and POPC molecules. The director vector of the cholesteryl ring moiety marked from C_B to C_A is also shown.

We analyzed the inter- and intramolecular properties of COs in a manner essentially similar to that previously used for a bulk CO system (20). Further details of the analysis methods are provided below and in the Supporting Material when necessary. We used 20 ns trajectory blocks to obtain error estimates for the calculated properties.

RESULTS AND DISCUSSION

Equilibration

We monitored the equilibration of the lipid droplet and trilayer systems by calculating the principal moments of inertia and the area per lipid as a function of time, respectively. These trajectories are shown in Fig. 2 and indicate equilibration after a period of ~30 ns for the droplet system and after ~80 ns for the trilayer system. Subsequent simulations were carried out for analysis purposes and lasted 60 ns for the droplet system and 80 ns for the trilayer system. We examined the equilibrium properties of the COs by calculating the radial distribution function (RDF) for the intermolecular O_A pairs and the COM of COs in 20 ns periods to check that no systematic drift was occurring after equilibration (data not shown).

The principal moments of inertia (I_x, I_y, and I_z) indicate that the shape of the lipid droplet fluctuates strongly during the equilibration period (see Fig. 2 *A*). Thereafter, the overall shape of the particle remains relatively spherical, although some fluctuations occur on the nanosecond scale. A representative snapshot in Fig. 2 *B* demonstrates the spherical shape of the particle.

To approximate the area per POPC molecule in the lipid droplet, we produced an RDF between the COM of POPCs and the COM of the droplet (see Fig. 3), which resulted in a radius of 3.34 nm. The approximate area per POPC of the droplet, A_{POPC}, was then ~0.78 nm^2. The radius of the lipid droplet was also determined by the average distance of a phosphorus atom of POPC from the COM of the lipid droplet. This was found to be 4 nm, which is in the range of the HDL particles (24). In the lamellar lipid trilayer system, A_{POPC} after equilibration was ~0.70 nm^2, which was calculated by dividing the *x-y* area of the system by the number of POPC molecules in one monolayer. The A_{POPC} in the trilayer is slightly more than the 0.68 nm^2 found in pure fluid POPC bilayers at a lower temperature of 310 K with the corresponding force field (25).

We also simulated a POPC bilayer at a temperature of 330 K to get an idea of the temperature dependence for different molecular properties. A_{POPC} in the bilayer simulation at 330 K was on average 0.69 ± 0.01 nm^2. Thus, COs do not induce a significant change in A_{POPC} in the trilayer system, which implies that if COs interdigitate into the hydrocarbon and headgroup regions of the monolayers, this effect is not very significant. This matter is discussed in more detail below.

Snapshots from the end of the simulations shown in Fig. 2 *B* indicate that the lipid droplet shrinks during equilibration and the dimensions of the trilayer system also slightly decrease. To study the effect of the starting configuration on the mixing of lipids in our systems, we carried out an

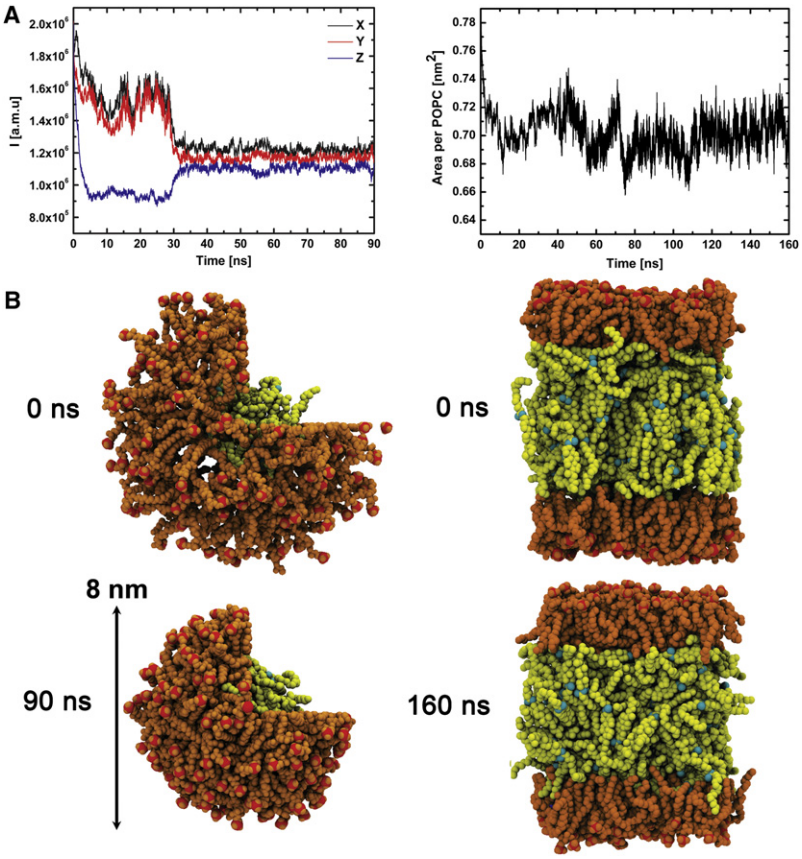

FIGURE 2 (*A*) Principal moments of inertia (*left*) and area per POPC molecule (*right*) profiles of the droplet and trilayer systems, respectively. The first 30 ns and 80 ns of the simulations were not included in the analysis. (*B*) Snapshots from the start and end of the simulations for the droplet (*left*) and trilayer (*right*). Molecules are visualized by means of van der Waals radii. The POPC molecules are shown in orange and red (nitrogen atoms), and the CO molecules appear in yellow and cyan (oxygen atoms). For clarity, water molecules are not shown. Pictures were produced using the VMD visualization program (40).

additional simulation for the lipid droplet. We initially placed six CO molecules outside of the particle (see the snapshots in the Supporting Material). During the first 5 ns of the simulation, the COs diffused from outer regions of the lipid droplet to the core. This indicates that the mixing of COs and POPCs was well equilibrated in our simulations, or that the systems were at least under near-equilibrium conditions where the partitioning of CEs converged, indicating their preference to reside in the core of the particle. Our recent coarse-grained simulations of lipid droplets and HDL particles are in agreement with this view (T. Murtola, T. Vuorela, P. Niemelä, A. Catte, A.S. Koivuniemi, M.T. Hyvönen, and I. Vattulainen, unpublished).

Molecular and atomic distributions

The mass density profiles of various molecules and atoms along the trilayer normal are shown in Fig. 3 together with the RDFs of POPC and CO atoms with respect to the COM of the lipid droplet. In addition, 2D number-density maps for the phosphorous atom of POPCs, whole POPC molecules, and the O_A and C_C atoms of COs are shown in Fig. 3.

The density profiles of the POPC molecules in the trilayer system show that the shape of the distribution profile for POPC remarkably resembles the profile in the POPC bilayer systems, with a peak at the PC headgroup region and shoulders approximately at the regions of carbons 3–8 of the chains (for numbering of the carbons, see Fig. 1). The distributions of CO molecules in the trilayer appear in two shallow peaks between the POPC regions, which may refer to a smectic-like orientation of COs in the core compartment, although the possible strata cannot be found by visual inspection. A more careful examination of the different regions of the CO molecules indicates that the densities of the oxygen atoms O_A and O_B of CO form peaks symmetrically at ~$\pm$1.3 nm. Furthermore, the density profiles of the C_C and C_D atoms, i.e., the opposite ends of the CO molecules, remarkably resemble each other, with three peaks at ~0 and $\pm$2.3 nm, whereas the methyl ends of the oleate chains (C_C) in COs tend to extend slightly further toward the water phase than the other ends of the CO molecules (C_D), indicating that acyl chains of COs are to some extent interdigitating with the acyl chains of POPCs. The density profile of C_A is more even but also shows four shallow peaks.

In the case of the small droplet, the RDFs and 2D number-density maps reveal that oxygen atoms of COs are distributed inside the hydrophobic CO core (shell peaks at ~0.2 nm in the RDF profile) of the droplet, whereas the C_C and C_D atoms are located further away (shell peaks at ~2 nm in the RDF profile). As in the trilayer, in the droplet the methyl ends of oleate chains (indicated by the RDFs of

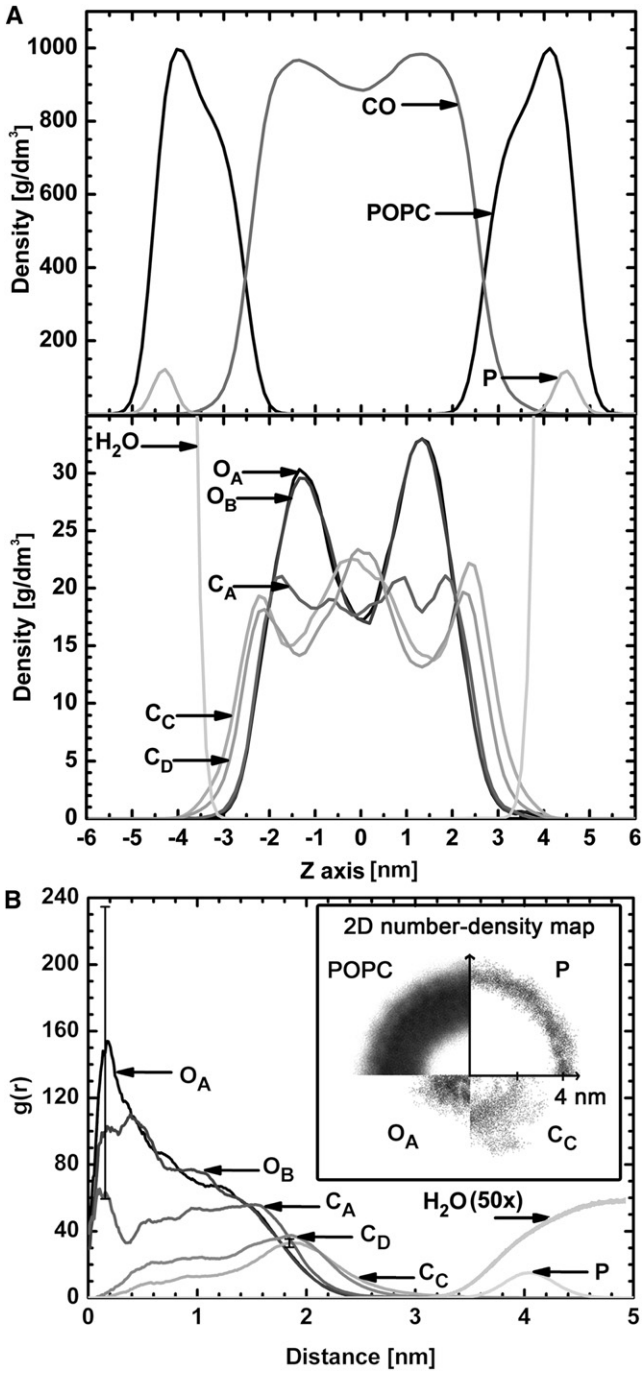

FIGURE 3 (*A*) Density profiles of the trilayer system for CO and POPC molecules together with phosphorus (P) atoms (*upper panel*). In addition, distributions are plotted for certain CO atoms and water molecules (*lower panel*). (*B*) RDFs and 2D number-density map (*inset*) for the different CO and POPC atoms and POPC molecules with respect to the COM of the lipid droplet.

C_C) in COs also extend further toward the surface of the droplet interdigitating with the acyl chains of POPCs.

The results indicate that the CO molecules are not randomly oriented, but form a weakly ordered smectic-like structure between the POPC monolayers in the trilayer system with ~3 nm separation of the shallow main peaks of CO. In the small droplet system, the space in the core was so limited and the number of core CO molecules so low that a similar double-layered structure was not registered. However, the ends of the acyl chains of COs were interdigitating with surface POPCs as in the case of the planar trilayer.

Of interest, calorimetric and small-angle x-ray scattering analyses of the core of LDL suggest that below the transition temperature, CEs form concentric shells (26) and are radially aligned (27,28). Our results suggest that a similar weak orientation ordering of COs could be possible even above the transition temperature. However, we have to keep in mind that the weak orientation order of the CO phase was seen in our lamellar trilayer system, which, in contrast to lipoproteins and lipid droplets, is not a spherical system. Furthermore, the presence of triglyceride molecules in physiological lipoproteins could destabilize the ordering between CO molecules. It was previously proposed that the acyl chains of surface phospholipids and core CEs interdigitate (29,30). In our simulations, this was also found to be the case.

Solubility of COs into POPC monolayers

To obtain useful approximate measures of the solubility of COs into the POPC monolayer in the simulations, we determined 1), the average mass of COs that interdigitated with POPC molecules; and 2), the number of hydrogen bonds formed by the oxygen atoms of CO and the water molecules (in several experimental studies, the interaction of CO oxygens with water molecules was used as a criterion for solubility (10,11)).

According to criteria 1, the solubility of CO in our trilayer system is 7 weight % (~8 mol %). To apply criteria 2, we found only one occurrence in each simulation, where the oxygens of COs are forming hydrogen bonds with water molecules. A hydrogen bond was determined when the distance between the O_A or O_B atoms of CO and the hydrogen atoms of water molecules was <0.18 nm (acceptor-hydrogen distance), and the angle associated with the acceptor-hydrogen-donor configuration was $<30°$. CO molecules formed hydrogen bonds with water molecules in time intervals of ~7 and ~40 ns in the droplet and trilayer systems, respectively. After a short prevalence at the surface, the CO molecules diffused back into the CO-rich region. Based on criterion 2, the solubility of CO is no more than 1:128, i.e., ~0.8 mol %.

The solubility of CEs into the lamellar structure of phospholipids was previously elucidated by means of ^{13}C NMR (10,11), surface pressure-area isotherms (31), and x-ray studies (9). In those studies, CEs were found to be slightly soluble into phospholipid surfaces. ^{13}C NMR studies typically indicate a solubility of 2–3 mol % CO to egg PC (which has POPC as the main component) at temperatures ranging from 25°C to 55°C (i.e., below the temperature of the simulations presented here), whereas studies based on pressure-area

isotherms indicate a solubility of 1.8 mol % CEs to POPC in 24°C. In the ^{13}C NMR studies, the criteria for the solubility of CEs was the amount of interaction between the ester oxygens of CEs and water molecules indicated by the differences in the chemical shifts of the ester bond oxygens of bulk and surface CEs. Earlier experimental approximations based on x-ray diffraction indicated the solubility of cholesteryl linolenate (18:3) to egg PC in the range of 3.1–4.5 mol % in 24°C depending on water concentration. Furthermore, in that study the solubility of cholesteryl linolenate into egg PC was based on the area per lipid calculations where approximate areas for different lipid components were chosen. In our trilayer simulation, CO molecules did not have a significant effect on the area per lipid of POPC, as mentioned above, although there was interdigitation between the CO and POPC molecules. In addition to the amount of water, the solubility is strongly affected by the properties of the environment, as well as the details of the structure in CE and phospholipid. Therefore, the values given above are not directly comparable, but they do show that the solubility of CO to POPC in the simulations is in the right ballpark. We have to keep in mind that during our simulations only one CO molecule diffused to the surface in both simulations, and thus it is very challenging to determine statistically accurate estimates for the solubility of CO based on criterion 2.

Intermolecular ordering of COs

The intermolecular orientational order parameter S_{RR} between the directors of COs (defined as the C_B-C_A vector; see Fig. 1) was determined in a manner similar to that previously described for an isotropic CO system (20). The S_{RR} profile describes the orientational correlation of CO ring moieties as a function of distance. CO shows similar intermolecular behavior in our POPC-CO systems, indicating that the cholesteryl ring moieties prefer to stack together at short intermolecular distances. This correlation vanishes at longer distances, indicating a liquid phase. Further discussion and details of the S_{RR} profile calculations are given in the Supporting Material.

Intramolecular properties

We calculated the probability distribution of the angle between the phosphorus-nitrogen (P-N) vector of the headgroup and the local normal of the system. The distributions show that the prevailing orientation of the headgroup is slightly more toward the water phase in the small lipid droplet. We also determined the probability distribution of the intramolecular angles between the oleate chain or the short acyl chain and the cholesterol director of CO as in our previous study of bulk CO (20). The distribution of the angles between the chains and the ring structure of CO is similar to that in the isotropic system (20), indicating that COs prefer elongated conformations, although bent horseshoe-type conformations were also registered. The probability distribution profiles and a more detailed discussion are given in the Supporting Material.

Ordering of acyl chains and cholesterol director

The order profiles of 16:0 and 18:1 chains of POPCs in the droplet and trilayer are plotted in Fig. 4. In the trilayer, the order parameters of the 16:0 and 18:1 chains closely resemble those obtained in the simulation of a pure POPC bilayer at a lower temperature (25) and observed in ^{2}H NMR studies (32). In addition, in the trilayer system the deuterium order parameters of the POPCs are identical to the ones found in the pure POPC bilayer simulation, which was done for comparison purposes at a temperature of 330 K (data not shown) to determine whether COs decrease the order parameters of the acyl chains of POPCs to the same level as observed in previous studies at lower temperatures. The 16:0 order parameters of POPC molecules in the small lipid droplet are clearly more disordered than the ones in the trilayer at the beginning of the chains, after which they slightly approach the trilayer order parameters toward the chain ends. Methylene segments C2–C9 of the 18:1 chains of the POPCs in the droplet are also strongly more disordered compared to the trilayer case. The shape of the double-bond region of the 18:1 chain differs between the systems: in the droplet, the carbon segment C9 is more disordered than

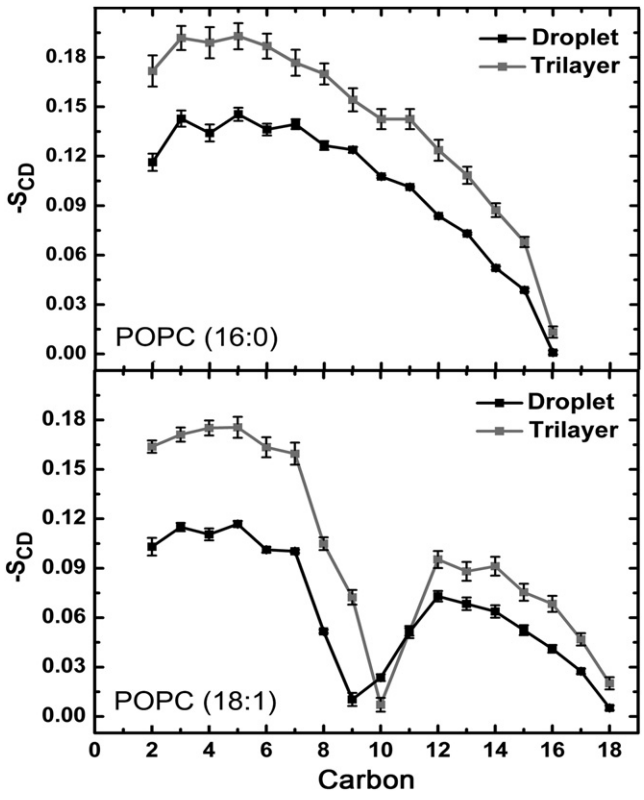

FIGURE 4 Deuterium order parameters of the acyl chains of POPC molecules in the droplet and trilayer for the *sn*-1 16:0 chain (*upper panel*) and *sn*-2 18:1 chain (*lower panel*).

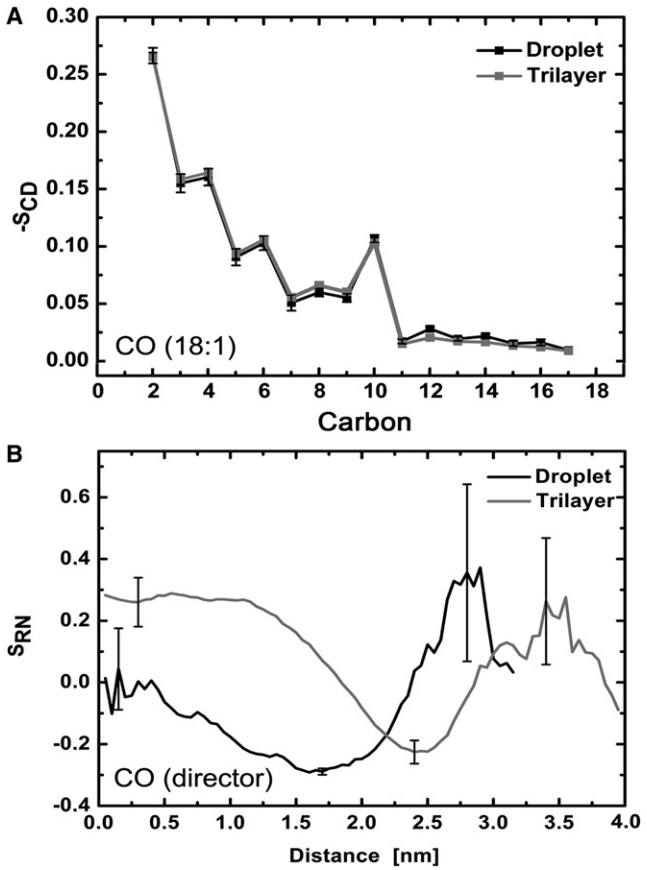

FIGURE 5 (*A*) 18:1-chain order parameters of CO with respect to the cholesterol director. (*B*) The order parameter profile of the cholesterol director with respect to the normal of droplet or the trilayer as a function of distance from the COM or the central *x*, *y* plane, respectively.

C10, whereas the opposite setting is observed in the trilayer. The minimum value is nearly the same in both systems. After the double-bond region, the difference between the systems becomes smaller. The results can be understood by realizing that the A_{POPC} is larger in the droplet than in the trilayer case, and thus the chains are more disordered because they try to minimize the hydrophobic surface that is in contact with the water phase.

Fig. 5 shows order parameters for the oleate chain (18:1) carbons of CO with respect to the CO director. The order parameters are similar to those found for an isotropic CO system in our earlier study (20). The C2–C10 carbons of the 18:1 chain are clearly more ordered than the C11–C17 carbons. The stacking of cholesterol bodies and acyl chains of COs could induce this effect. Fig. 5 also shows the order parameter, S_{RN}, of the cholesterol director with respect to the local normal. It indicates isotropic orientation with respect to the normal of the system near the COM of the lipid droplet, whereas the orientation shifts to a more perpendicular one when the distance of CO increases from the COM. Finally, when CO is located in the POPC monolayer (rare event, large error bars), the conformation of the director is merely parallel to the normal. In the trilayer case, the orientation of the CO director is more parallel with respect to the normal near the geometrical *x*, *y* plane, and with increasing distance a structural behavior similar to that observed in the case of the lipid droplet is observed.

What is remarkable is that the CO molecules do not induce any changes in the order parameters of POPCs, although the CO molecules ''sense'' the POPC monolayers at least by their cholesteryl ring moieties, as indicated by the S_{RN} profiles. This kind of orientational ordering at the phospholipid-cholesterol ester interfaces has not yet been observed experimentally. This is intriguing because, at the phase transition temperature, the CE compartments in the lipoproteins and lipid droplets are more ordered, and thus the orientation behavior of CEs found here could be absent at the POPC-CO interface, which again could play a critical role in CE transport and hydrolysis.

Angle distribution of the CO director with respect to normal of the trilayer

The distribution of the angle between the CO director and the trilayer normal as a function of distance from the geometrical *x*, *y* plane of the trilayer is shown in Fig. 6. The angle shifts from parallel to more perpendicular with respect to the normal of the trilayer as COs closer to the phospholipid surface are monitored. This behavior was also seen in the director order profiles in Fig. 5. To determine whether the conformation of CO changes in accordance with the results shown in Figs. 5 and 6, we probed the time evolution of the angle of one individual CO that forms hydrogen bonds with water molecules according to criterion 2 described above. Of interest, when the CO is located in the core region, it adopts small angles, whereas at the POPC-CO interface the director angle with respect to the normal changes to ~90°.

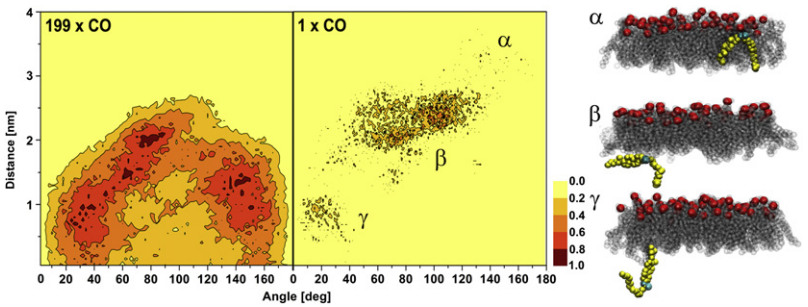

FIGURE 6 Angle distribution of the cholesterol sterol body with respect to the trilayer normal as a function of distance from the central *x*, *y* plane of the trilayer for all COs (*left panel*) and separately for one CO (*middle panel*). Three snapshots are shown for the CO, the angle of which was probed separately. The approximate locations of the snapshots in the angle distribution are also marked. POPCs are colored in black, nitrogen atoms of POPCs in red, the CO in yellow, and the oxygen atoms of the CO in cyan.

Finally, when the CO is solubilized into a POPC monolayer, the angle ranges from 140° to 160°. This behavior is very similar to the phenomena observed in the S_{RN} profile. It should be noted that the snapshots from the simulation trajectory are not in chronological order. Further, after the CO localized to the surface, it diffused back to the POPC-CO interface and finally back to the CO core.

We conclude that the CE molecules likely penetrate into the phospholipid monolayer with the help of ester bond regions, which interact by dipole-dipole interactions with water molecules and the polar regions of phospholipids. An energy barrier likely is involved in the localization of CE molecules into phospholipid monolayers, and the height of the barrier presumably depends on various factors, such as the number and composition of lipids in the surrounding monolayer.

Conformation of COs at surface phase

Various groups have studied and speculated on the conformation of CEs in phospholipid surfaces (11,31,33,34). The predominant idea is that when CEs interact with water molecules through ester oxygens, they adapt a horseshoe-like conformation. In the horseshoe conformation, a given acyl chain and cholesteryl moiety orient toward the lipid interior, and the ester bond oxygens of the CEs interact with water molecules. Since the conformation of CE at the surface regions (e.g., in lipoproteins) is most likely important for the activity of carrier proteins and hydrolyzing enzymes, we elucidated the conformations of COs during the events in which the ester bond oxygens of CO molecules formed hydrogen bonds with water molecules. That is, we used the same events as before to estimate the solubility of CO molecules into POPC monolayers according to criterion 2.

In the trilayer simulation, within the 40 ns time frame, the surface orientation of CO in the POPC monolayer fluctuated between the previously proposed horseshoe conformation and a more extended conformation at the surface (data not shown). During the short 7 ns visit of one CO at the surface region of the droplet, almost only extended (not horseshoe) CO conformations were registered, with an acyl chain located in the water-lipid interface. This may be related to the higher curvature of the droplet. In the trilayer system, the surface conformations of CO agree with the conformations based on similar experimental systems. It is noteworthy, however, that we also found more extended conformations, especially in the case of higher curvature, which may play an important role in CE metabolism. This is discussed in more detail elsewhere. It should be noted that only one CO molecule was localized to the surface in each simulation, which makes it difficult to draw solid statistically significant conclusions from the results.

CONCLUSIONS

In this study we unraveled the structural properties of two lipid systems composed of POPC and CO molecules—a small (approximately HDL-sized) lipid droplet and a lamellar lipid trilayer—by utilizing atomic-scale molecular-dynamics simulations.

In both the droplet and the trilayer, the POPC molecules encapsulated the CO molecules and both species of molecules were located in separate phases, with some interdigitation between the acyl chains at the interfacial regions. In the interior of the trilayer, the CO molecules formed two slightly denser strata that arose from the oxygen atoms of the ester bond, suggesting that smectic-like phase behavior could exist above the phase transition temperature of CO molecules. The deepest core of the small droplet contained predominantly ester bond regions of the COs, whereas both ends of the COs interacted with the POPCs of the surface.

In reasonable accordance with experiments, the simulations imply a low solubility of a few mol % of COs into the POPC layer. It is important to note that localization of CEs into the phospholipid monolayer is probably a relatively rare event, which precludes accurate measurements of the solubility during short simulation times as in this study. Concerning ordering in the simulated systems, the order parameters of the POPC acyl chains in the trilayer were found to be similar to those in the POPC bilayer simulation and in previous NMR studies. However, in the lipid droplet the acyl chains of POPC molecules were clearly more disordered than in the trilayer and POPC bilayer systems. Also, the orientational behaviors of the phosphocholine headgroups in the droplet and trilayer systems differed in that the most prevailing orientation in the droplet was shifted slightly toward the water phase as compared to the trilayer and POPC bilayer systems. Regarding the ordering of CO molecules, the cholesteryl ring moieties preferred to stack together at short intermolecular distances, but this correlation vanished at longer distances, indicating the liquid phase. CO molecules preferred elongated conformations, although bent horseshoe-type conformations were also registered. The ordering of the CO director with respect to the local normal of the system was computed as a function of the distance from the COM of the droplet or the central x, y plane of the trilayer. Deep in the core of the small droplet or trilayer, the orientation was merely isotropic or slightly parallel to the normal, respectively. At the CO-POPC interface the orientation shifted toward perpendicular and, finally, the low prevalence of the COs in the POPC monolayer showed an orientation that allowed the ester bond region of COs to interact with the water molecules. It should be noted that our lipid droplet is on the size scale of the smallest HDL particles (7–12 nm) and thus the CO core is small compared to larger lipoproteins and lipid droplets. It is possible that in the larger lipoproteins and lipid droplets the CEs are ordered as in our trilayer case (with no curvature and a bulkier CO phase), in which the CO directors preferably orient slightly parallel to the normal of the trilayer and form denser strata by the oxygen atoms. Indeed, this kind of lamellae-like behavior has been

registered by electron cryomicroscopy under the phase transition temperature of the core of LDL particles (35).

Apolipoproteins (e.g., apolipoprotein B-100 (apoB-100) and apolipoprotein A-I (apoA-I)) play a very important role in the ordering and stabilization of lipoproteins, and thus many of the properties discussed here could be modulated by different apolipoproteins as well as by other proteins capable of binding lipoproteins (36–38). However, in this study our goal was first to understand how the different lipid components behave without the protein environment. In future work, we will study more complex lipoprotein or lipid droplet systems.

Earlier experimental studies suggested that the horseshoe conformation is the most prevailing conformation of CEs at the phospholipid-water interface. In this conformation, the acyl chain is bent to lie next to the cholesterol body while the ester bond region interacts with water molecules. The simulations presented here indicated more flexibility for the conformation of the COs, allowing more extended conformations in the POPC monolayer, although horseshoe-like features were also found. From a metabolic point of view, the solubilization of CEs into phospholipid monolayers and the conformations of CEs within the monolayer are likely to be important regulatory factors of CE transportation and hydrolysis inasmuch as they determine the interaction between CEs and the cholesterol ester transfer protein (CETP) and cholesteryl esterases. The crystal structure of CETP (39) reveals two CO molecules in extended conformation, indicating that CE molecules enter the hydrophobic cavity of the CETP with the acyl chain or the cholesterol body first, and that CETP may favor more flexible conformations of CEs within phospholipid monolayers.

Taken together, these results underline the importance of atomic-scale molecular-dynamics simulations for revealing details about complex lipid mixtures and elucidating experimentally observed phenomena. This work lays the basis for further simulation studies related to more complex lipoprotein and lipid droplet systems; however, such studies will also require the use of coarse-grained models in dynamic simulations.

SUPPORTING MATERIAL

Additional text, figures, and references are available at http://www.biophysj.org/biophysj/supplemental/S0006-3495(09)00656-0.

The Wihuri Research Institute is maintained by the Jenny and Antti Wihuri Foundation. We thank the Finnish IT Center of Scientific Computing for providing computational resources.

This study was supported by the Emil Aaltonen Foundation (A.K.) and the Academy of Finland (A.K., M.T.H., and I.V.).

REFERENCES

1. Ikonen, E. 2008. Cellular cholesterol trafficking and compartmentalization. *Nat. Rev. Mol. Cell Biol.* 9:125–138.
2. Hevonoja, T., M. O. Pentikainen, M. T. Hyvonen, P. T. Kovanen, and M. Ala-Korpela. 2000. Structure of low density lipoprotein (LDL) particles: basis for understanding molecular changes in modified LDL. *Biochim. Biophys. Acta.* 1488:189–210.
3. Brown, M. S., and J. L. Goldstein. 1983. Lipoprotein metabolism in the macrophage: implications for cholesterol deposition in atherosclerosis. *Annu. Rev. Biochem.* 52:223–261.
4. Martin, S., and G. Parton. 2006. Lipid droplets: a unified view of a dynamic organelle. *Nature.* 7:373–378.
5. Zhao, B., B. J. Fisher, R. W. St Clair, L. L. Rudel, and S. Ghosh. 2005. Redistribution of macrophage cholesteryl ester hydrolase from cytoplasm to lipid droplets upon lipid loading. *J. Lipid Res.* 46:2114–2121.
6. Adorni, M. P., F. Zimetti, J. T. Billheimer, N. Wang, D. J. Rader, et al. 2007. The roles of different pathways in the release of cholesterol from macrophages. *J. Lipid Res.* 48:2453–2462.
7. Brasaemle, D. L. 2007. Thematic review series: adipocyte biology. The perilipin family of structural lipid droplet proteins: stabilization of lipid droplets and control of lipolysis. *J. Lipid Res.* 48:2547–2559.
8. Tauchi-Sato, K., S. Ozeki, T. Houjou, R. Taguchi, and T. Fujimoto. 2002. The surface of lipid droplets is a phospholipid monolayer with a unique fatty acid composition. *J. Biol. Chem.* 277:44507–44512.
9. Janiak, M. J., C. R. Loomis, G. Shipley, and D. M. Small. 1974. The ternary phase diagram of lecithin, cholesteryl linolenate and water: phase behavior and structure. *J. Mol. Biol.* 86:325–339.
10. Spooner, P. J. R., J. A. Hamilton, D. L. Gantz, and D. M. Small. 1986. The effect of free cholesterol on the solubilization of cholesteryl oleate in phosphatidylcholine bilayers: a 13C-NMR study. *Biochim. Biophys. Acta.* 860:345–353.
11. Hamilton, J. A., and D. M. Small. 1982. Solubilization and localization of cholesteryl oleate in egg phosphatidylcholine vesicles. A carbon 13 NMR study. *J. Biol. Chem.* 13:7318–7321.
12. Glick, J. M., S. J. Adelman, M. C. Phillips, and G. H. Rothblat. 1983. Cellular cholesteryl ester clearence. relationship to the physical state of cholesteryl ester inclusions. *J. Biol. Chem.* 258:13425–13430.
13. Small, D. M., and G. G. Shipley. 1984. Physical-chemical basis of lipid deposition in atheroclerosis. *Science.* 185:222–229.
14. Catte, A., J. C. Patterson, M. K. Jones, F. Gu, L. Li, et al. 2008. Structure of spheroidal HDL particles revealed by combined atomistic and coarse-grained simulations. *Biophys. J.* 94:2306–2319.
15. Shih, A. Y., S. G. Sligar, and K. Schulten. 2008. Molecular models need to be tested: the case of a solar flares discoidal HDL model. *Biophys. J.* 94:87–89.
16. Shih, A. Y., P. L. Freddolino, A. Arkhipov, and K. Schulten. 2007. Assembly of lipoprotein particles revealed by coarse-grained molecular dynamics simulations. *J. Struct. Biol.* 157:579–592.
17. Shih, A. Y., I. G. Denisov, J. C. Phillips, S. G. Sligar, and K. Schulten. 2004. Molecular dynamics simulations of discoidal bilayers assembled from truncated human lipoproteins. *Biophys. J.* 88:548–556.
18. Smith, E. B. 1974. The relationship between plasma and tissue lipids in human atherosclerosis. *Adv. Lipid Res.* 12:1–49.
19. Kupiainen, M., E. Falck, S. Ollila, A. A. Gurtovenko, M. T. Hyvönen, et al. 2005. Free volume properties of sphingomyelin, DMPC, DPPC, and PLPC bilayers. *J. Comput. Theor. Nanosci.* 2:401–413.
20. Heikelä, M., I. Vattulainen, and M. T. Hyvönen. 2005. Atomic simulation studies of cholesteryl oleates: model for the core of lipoprotein particles. *Biophys. J.* 90:2247–2257.
21. Lund-Katz, S., L. Liu, T. Thuahnai, and M. C. Phillips. 2003. High density lipoprotein structure. *Front. Biosci.* 8:d1044–d1054.
22. Tieleman, D. P., M. S. P. Sansom, and H. J. C. Berendsen. 1999. Alamethicin helices in a bilayer and in solution: molecular dynamics simulations. *Biophys. J.* 76:40–49.
23. Hess, B., C. Kutzner, D. van der Spoel, and E. Lindahl. 2008. GROMACS 4: algorithms for highly efficient, load-balanced, and scalable molecular simulation. *J. Chem. Theory Comput.* 4:435–447.
24. Colhoun, H. M., J. D. Otvos, M. B. Rubens, M. R. Taskinen, S. R. Underwood, et al. 2002. Lipoprotein subclasses and particle sizes

and their relationship with coronary artery calcification in men and women with and without type 1 diabetes. *Diabetes*. 51:1949–1956.

25. Ollila, S., M. T. Hyvonen, and I. Vattulainen. 2007. Polyunsaturation in lipid membranes: dynamic properties and lateral pressure profiles. *J. Phys. Chem. B*. 111:3139–3150.
26. Deckelbaum, R. J., G. G. Shipley, and D. M. Small. 1977. Structure and interactions of lipids in human plasma low density lipoproteins. *J. Biol. Chem.* 252:744–754.
27. Laggner, P., G. M. Kostner, G. Degovics, and D. L. Worcester. 1984. Structure of the cholesteryl ester core of human plasma low density lipoproteins: selective deuteration and neutron small-angle scattering. *Proc. Natl. Acad. Sci. USA*. 81:4389–4393.
28. Baumstark, M. W., W. Kreutz, A. Berg, I. Frey, and J. Keul. 1990. Structure of human low-density lipoprotein subfractions, determined by X-ray small-angle scattering. *Biochim. Biophys. Acta*. 1037:48–57.
29. Laggner, P., and K. W. Muller. 1978. The structure of serum lipoproteins as analysed by x-ray small-angle scattering. *Q. Rev. Biophys.* 3:371–425.
30. Ginsburg, G. S., D. M. Small, and D. Atkinson. 1982. Microemulsions of phospholipids and cholesterol esters. *J. Biol. Chem.* 257:8216–8227.
31. Smaby, J. M., and H. L. Brockman. 1987. Acyl unsaturation and cholesteryl ester miscibility in surfaces. formation of lecithin-cholesteryl ester complexes. *J. Lipid Res.* 28:1078–1087.
32. Huber, T., K. Rajamoorthi, V. Kurze, K. Beyer, and M. F. Brown. 2002. Structure of docosahexaenoic acid-containing phospholipid bilayers as studied by 2H NMR and molecular dynamics simulations. *J. Am. Chem. Soc.* 124:298–309.
33. Salmon, A., and J. A. Hamilton. 1995. Magic-angle spinning and solution 13C nuclear magnetic resonance studies of medium- and long-chain cholesteryl esters in model bilayers. *Biochemistry*. 34:16065–16073.
34. Grover, A. K., B. J. Forrest, R. K. Buchinski, and R. J. Cushley. 1979. ESR studies on the orientation of cholesteryl ester in phosphatidylcholine multilayers. *Biochim. Biophys. Acta*. 550:212–221.
35. Orlova, E. V., M. B. Sherman, W. Chiu, H. Mowri, L. C. Smith, et al. 1999. Three-dimensional structure of low density lipoproteins by electron cryomicroscopy. *Proc. Natl. Acad. Sci. USA*. 96:8420–8425.
36. Marcel, Y. L., and R. S. Kiss. 2003. Structure-function relationships of apolipoprotein A-I: a flexible protein with dynamic lipid associations. *Curr. Opin. Lipidol.* 14:151–157.
37. Segrest, J. P., M. K. Jones, H. De Loof, and N. Dashti. 2001. Structure of apolipoprotein B-100 in low density lipoproteins. *J. Lipid Res.* 42:1346–1367.
38. Segrest, J. P., L. Li, G. M. Anantharamaiah, S. C. Harvey, K. N. Liadaki, et al. 2000. Structure and function of apolipoprotein A-I and high-density lipoprotein. *Curr. Opin. Lipidol.* 11:105–115.
39. Qiu, X., A. Mistry, M. J. Ammirati, B. A. Chrunyk, R. W. Clark, et al. 2007. Crystal structure of cholesteryl ester transfer protein reveals a long tunnel and four bound lipid molecules. *Nat. Struct. Mol. Biol.* 14:106–113.
40. Humphrey, W., A. Dalke, and K. Schulten. 1996. VMD: visual molecular dynamics. *J. Mol. Graph.* 14:33–38.